

# Broadband optical frequency comb generation with a phase-modulated parametric oscillator

Scott A. Diddams, Long-Sheng Ma,\* Jun Ye, and John L. Hall

*JILA, University of Colorado, and National Institute of Standards and Technology, Boulder, Colorado 80309-0440*

Received August 5, 1999

We introduce a novel broadband optical frequency comb generator consisting of a parametric oscillator with an intracavity electro-optic phase modulator. The parametric oscillator is pumped by 532-nm light and produces near-degenerate signal and idler fields. The modulator generates a comb structure about both the signal and the idler. Coupling between the two families of modes results in a dispersion-limited comb that spans 20 nm (5.3 THz). A signal-to-noise ratio of >30 dB in a 300-kHz bandwidth is observed in the beat frequency between individual comb elements and a reference laser. © 1999 Optical Society of America

OCIS codes: 190.2620, 120.3940.

Traditional optical frequency combs are made by placing an electro-optic modulator (EOM) inside a resonant optical cavity.<sup>1,2</sup> The light from an external laser, which can be stabilized at the hertz level to an atomic or molecular transition, is coupled into the cavity. The EOM is driven by a stable radio frequency (rf) or microwave oscillator at a frequency  $f_m$ , which is an integer multiple of a cavity free spectral range  $f_{\text{FSR}}$ . With moderate modulation index  $\beta$ , the EOM primarily shifts energy out of the carrier frequency into two adjacent sidebands at frequencies  $f_0 \pm f_m$ . These sidebands pass back through the EOM and generate secondary sidebands, which in turn generate their own resonant sidebands. Because of limits on cavity finesse ( $\mathcal{F}$ ) and  $\beta$ , this process gradually converges, and the power in the higher-order modes decreases exponentially. To a good approximation, the output power in the  $k$ th sideband is  $P_k \propto \exp[-|k|\pi/(\beta\mathcal{F})]$ .<sup>1</sup>

When it is operated with known values of the frequency of the input light and  $f_m$ , such an optical frequency comb generator is a valuable precision link between unknown optical frequencies and known standards separated by many terahertz.<sup>3,4</sup> However, the usable bandwidth of such a comb generator is typically restricted to ~5 THz by practical limits of the modulation index and cavity finesse, in addition to the dispersion of the cavity elements.<sup>5</sup> One attempt to overcome bandwidth limitations involved the insertion of dispersion-compensating prisms into the comb generator cavity.<sup>6</sup> In the 1.5- $\mu\text{m}$  regime, Imai *et al.* broadened the comb spectra to 50 THz by amplification and four-wave mixing in dispersion-shifted optical fiber.<sup>7</sup> In this Letter we demonstrate a new implementation of an optical frequency comb generator based on a phase-modulated optical parametric oscillator (OPO). As is shown below, the parametric gain relaxes the restrictions of high cavity finesse and modulation index while providing more flexibility to implement dispersion control.

The possibility of placing a source of conventional optical gain (e.g., electrically or optically pumped solid-state media) inside a comb generator was proposed by Ho and Kahn.<sup>8</sup> Our approach differs in that we use

parametric gain as provided by a phase-matched nonlinear crystal. Parametric gain has several unique advantages: (1) The parametric process is intrinsically broadband and tunable, as it does not depend on atomic or molecular resonances. (2) The parametrically generated photons are phase coherently linked to the pump field. (3) The parametric process is quiet, with the pump being the dominant noise source. However, rather than simply providing parametric gain for a conventional comb generator, we have chosen to create a near-degenerate OPO in which an intracavity EOM generates a family of sidebands about the signal and idler waves. This approach maintains the simplicity of a device that has a single-frequency input and multiple frequencies at the output. In what follows, we shall refer to this device and its output as an OPO comb.

The basic apparatus is shown in Fig. 1. Single-frequency light at 532 nm pumps the parametric oscillator, which employs 7.5 mm of type I MgO-doped LiNbO<sub>3</sub> as the gain medium ( $T = 108^\circ\text{C}$ ). The curved face ( $R = 10$  mm) of this crystal is coated to be a high reflector at both 532 and 1064 nm. The remainder of the cavity consists of two concave mirrors that have radii of curvature of 15 cm (M1) and 25 cm (M2), and a flat mirror (M3). Mirror M3, with high transmission at 532 nm, is added to the cavity to remove the green light trapped by the nonideal 30% reflectivity of M1 at 532 nm. All mirrors are high reflectors at 1064 nm, but leakage through M3 is used for diagnostics.

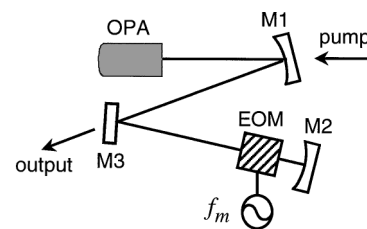


Fig. 1. Experimental apparatus: OPA, hemilithic MgO:LiNbO<sub>3</sub> optical parametric amplifier; EOM, MgO:LiNbO<sub>3</sub> EOM. See text for details.

Mirror M2 is mounted upon a piezoelectric transducer for fine control of the cavity length, although active stabilization is not employed. A lumped-circuit resonant EOM,<sup>9</sup> consisting of a 2 mm × 2 mm × 20 mm piece of MgO-doped LiNbO<sub>3</sub>, is placed at the position of the second beam waist near mirror M2. The EOM is tuned to be resonant at the cavity frequency (~350 MHz), and 0.35 rad of phase modulation is obtained with 200 mW of applied rf power.

With no rf power applied to the EOM, the loaded, unpumped cavity of Fig. 1 has  $\mathcal{F} = 150$ . The minimum pump threshold for near-degenerate parametric oscillation is ~200 mW (measured between M1 and the gain crystal). At a pump power 2.5× above threshold, the spectra of Fig. 2 were recorded with a grating-based optical spectrum analyzer. Figure 2(a) shows the near-degenerate oscillation of both the signal and the idler. Driving the EOM with 200 mW of rf power yields the spectrum of Fig. 2(b), where we see significant spectral broadening about the signal and idler. An increase of the cavity length by a fraction of the resonant wavelength acts to move the signal and idler branches of the spectrum together. When the two branches meet, as shown in Fig. 2(c), some interference-like oscillations in the spectrum are commonly seen. However, the two branches then lock together to form a single broadband comb spanning 18 nm, as shown in Fig. 2(d). The device operates stably in this fashion for hours, although the width of the spectrum depends on variations in the cavity length. With a doubling of the rf power to the modulator ( $\beta = 0.5$ ), we obtain the spectra of Figs. 2(e) and 2(f); in these two figures we also point out the hysteresis in the behavior of the system. Once the signal and the idler branches of the spectrum have been locked together, the cavity length can be decreased on a submicrometer scale to spread the spectrum to greater widths. This is the case in going from Fig. 2(e) to Fig. 2(f). A further decrease in the cavity length results in the marginally stable spectrum of Fig. 2(f) again splitting into two separate signal and idler branches.

Two of the most interesting features of the data of Fig. 2(e) are the relatively small variations in power across the spectrum and the sharp cutoff at the edges. Assuming a conventional comb generator without gain and using the values of  $\beta = 0.5$  rad,  $\mathcal{F} = 150$ , and  $f_m = 350$  MHz, one predicts that the spectral power will decrease by 520 dB per THz. This is in marked contrast to the power variation of less than 15 dB seen across the 5.3-THz spectrum of Fig. 2(e). Clearly, the parametric gain plays a crucial role. Furthermore, one could expect additional significant gains by employing shorter cavities and higher modulation frequencies, thereby concentrating the energy of the current 15,000+ modes into 10 or 50 times fewer modes. Similar sharp spectral cutoffs, which are due to dispersive material in the cavity, have been observed and explained in conventional comb generators by Kouroggi *et al.*<sup>5</sup> An estimate of the dispersion-limited bandwidth can be made with the expression  $\Delta f_{\max} = [4\beta/(Lk_0''\pi^2)]^{1/2}$ , where  $k_0'' = d^2k/d\omega^2$  evaluated at the center comb frequency and  $L$  is the length of the intracavity material. For MgO:LiNbO<sub>3</sub> at  $\lambda_0 =$

1064 nm,  $k_0'' = 2745$  fs<sup>2</sup>/cm and  $k_0'' = 2390$  fs<sup>2</sup>/cm for the *o* and *e* waves, respectively. Using these values and the experimental parameters of Figs. 2(e)–2(f), one predicts a bandwidth of 5.4 THz, which agrees well with the experimental results. This analysis demonstrates that, in pushing for broader bandwidth, it will be crucial to minimize the cavity dispersion. The use of dispersion-compensating prisms or mirrors is an obvious step in this direction, and the presence of gain provides flexibility in dealing with the anticipated losses. Another promising approach is the simple reduction of cavity material by combining the parametric amplifier and the EOM in the same crystal.

The action of the EOM to distribute the parametrically generated energy among the various modes relaxes the normally stringent demands on the OPO cavity stability. Oscillation occurs on every mode over a significant bandwidth, and each mode is coupled to its nearest neighbors via the EOM and to its conjugate partner by means of the parametric interaction with the pump. Beyond output coupling, power is lost only in the wings of the spectrum, where dispersively shifted modes are no longer efficiently coupled. The result is a form of mode-locked operation with steady-state, spectrally integrated output shown in Fig. 3. The unstable (mode-hopping) output of the free-running OPO with the EOM turned off is shown in Fig. 3(a). However, when the EOM is turned on, the stability improves dramatically, as shown in Fig. 3(b). In this case  $f_m$  was detuned ~50 Hz above  $f_{\text{FSR}}$ . Further improvements in the stability are seen when  $f_m = f_{\text{FSR}}$ , as is the situation in Fig. 3(c). We note here that the detuning between  $f_m$  and  $f_{\text{FSR}}$  could be varied

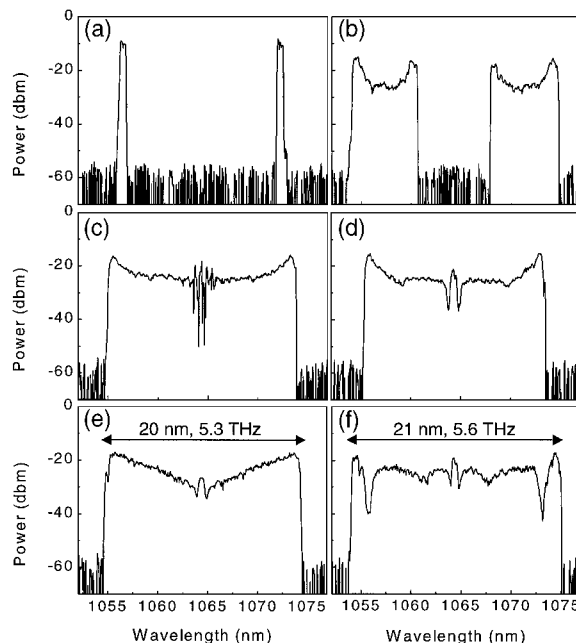


Fig. 2. (a) Near-degenerate parametric oscillation with the EOM off. (b) Comb output with the EOM on,  $\beta = 0.35$  rad. (c), (d) Comb output for two successively longer cavity lengths. (e), (f) Comb output with  $\beta = 0.5$  rad. The cavity length was decreased ~40 nm in going from (e) to (f). Resolution bandwidth is 0.5 nm.

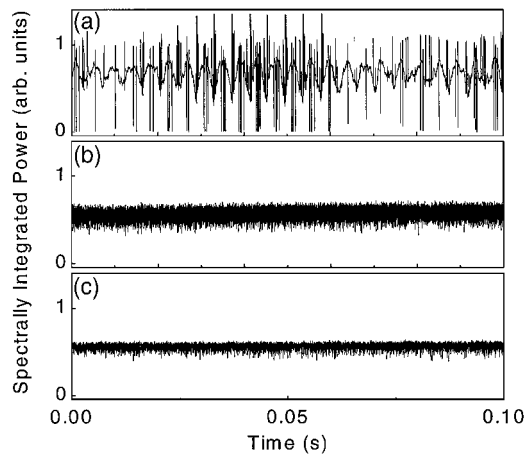


Fig. 3. Spectrally integrated output of the comb with (a) EOM off, (b) EOM on but  $f_m$  detuned slightly above  $f_{FSR}$ , and (c) EOM on with  $f_m = f_{FSR}$ . The standard deviations of the intensity fluctuations in these three cases are 23%, 9%, and 4% of the mean intensity, respectively. Detection bandwidth,  $\sim 1$  MHz.

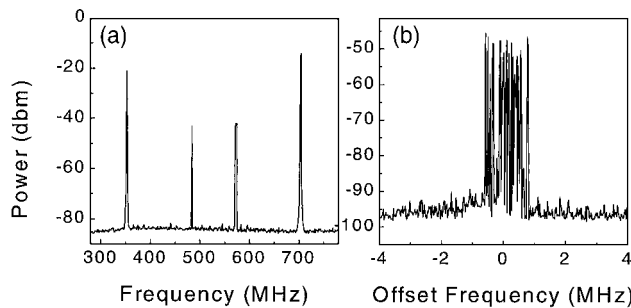


Fig. 4. (a) rf spectrum of the heterodyne signal between the OPO comb and a stable reference laser. The peaks at 350 and 700 MHz are the OPO-comb harmonics; the two smaller peaks are the heterodyne signal. Resolution bandwidth, 300 kHz. (b) Detailed view of the signal of (a) near 475 MHz. Resolution bandwidth, 10 kHz.

by  $\pm 5$  kHz before the increased losses terminated oscillation.

To verify that sharp comb lines indeed exist under the broad spectra of Figs. 2(d)–2(f) we have heterodyned the comb output with a stable, single-frequency Nd:YAG laser (linewidth,  $\leq 20$  kHz) operating at 1064 nm. The full OPO-comb output is combined with the Nd:YAG laser on an InGaAs P–I–N photodiode, and the resultant beat frequencies are recorded with a rf spectrum analyzer are presented in Fig. 4. Within the span of Fig. 4(a), we see both the intramode beats of the OPO comb at 350 and 700 MHz and the two weaker heterodyne signals from the interference between the Nd:YAG laser and adjacent elements of the OPO comb. Figure 4(b) shows one of the heterodyne signals in an 8-MHz window with a 10-kHz resolution bandwidth and a sweep rate of 1 MHz/20 ms. The signal remains sharp but shows variations of a few

megahertz in many tens of milliseconds, which we believe is largely the result of the frequency jitter on the OPO-comb pump.

An interesting question is whether the current OPO comb operates with an even or an odd number of modes. In the latter case one would find a mode at exact degeneracy ( $f_p/2$ ), whereas in the former case the modes would be split evenly about the frequency  $f_p/2$ . This question will need to be addressed if the full potential of the device is to be realized—for example, direct connection of every element of the comb to  $f_p$  and the well-known iodine transition at 532 nm.<sup>4</sup> Nonetheless, with precise knowledge of  $f_m$  the current device is already appropriate for measuring across large frequency gaps. In this regard, the spectroscopy of helium is an interesting field of study. A recent determination of the fine-structure splitting on the  $2^3S_1 \rightarrow 2^3P_J$  transition has prompted the further consideration of helium as a valuable system for measuring fundamental constants and testing QED.<sup>10</sup> With an increase in bandwidth, the OPO comb could prove valuable in this endeavor through the measurement of the absolute frequency of this 1083-nm transition by comparison with the 532–1064-nm standard.

The authors are grateful for the valuable insights and assistance of M. Raymer and A. Zozulya. Funding for this research was provided by the National Science Foundation and the National Institute of Standards and Technology, and S. A. Diddams is thankful for the support of the National Research Council. S. A. Diddams's e-mail address is sdiddams@jila.colorado.edu.

\*Permanent address, Laboratory for Quantum Optics, East China Normal University, Shanghai, China.

## References

1. M. Kourogi, K. Nakagawa, and M. Ohtsu, *IEEE J. Quantum Electron.* **29**, 2693 (1993).
2. L. R. Brothers, D. Lee, and N. C. Wong, *Opt. Lett.* **19**, 245 (1994).
3. A. Huber, Th. Udem, B. Gross, J. Reichert, M. Kourogi, K. Pachucki, M. Weitz, and T. W. Hänsch, *Phys. Rev. Lett.* **80**, 468 (1998).
4. J. L. Hall, L.-S. Ma, M. Taubman, B. Tiemann, F.-L. Hong, O. Pfister, and J. Ye, *IEEE Trans. Instrum. Meas.* **48**, 583 (1999).
5. M. Kourogi, B. Widiyatomo, Y. Takeuchi, and M. Ohtsu, *IEEE J. Quantum Electron.* **31**, 2120 (1995).
6. L. R. Brothers and N. C. Wong, *Opt. Lett.* **22**, 1015 (1997).
7. K. Imai, B. Widiyatomo, M. Kourogi, and M. Ohtsu, *IEEE J. Quantum Electron.* **35**, 559 (1999).
8. K.-P. Ho and J. M. Kahn, *IEEE Photon. Technol. Lett.* **5**, 721 (1993).
9. J. Kelley and A. Gallagher, *Rev. Sci. Instrum.* **58**, 563 (1987).
10. F. Minardi, G. Bianchini, P. Cancio Pastor, G. Giusfredi, F. S. Pavone, and M. Inguscio, *Phys. Rev. Lett.* **82**, 1112 (1999).